Technical University of Denmark

DTU

Sensitivity of resistive and Hall measurements to local inhomogeneities
Finite-field, intensity, and area corrections

Koon, Daniel W.; Wang, Fei; Petersen, Dirch Hjorth; Hansen, Ole

[Link back to DTU Orbit](#)

DTU Library
Technical Information Center of Denmark

Sensitivity of resistive and Hall measurements to local inhomogeneities: Finite-field, intensity, and area corrections

Daniel W. Koon, Fei Wang, Dirch Hjorth Petersen, and Ole Hansen

---

Articles you may be interested in

Sensitivity of resistive and Hall measurements to local inhomogeneities
J. Appl. Phys. **114**, 163710 (2013); 10.1063/1.4826490

Correction for thermal lag in dynamic temperature measurements using resistance thermometers
Rev. Sci. Instrum. **84**, 074903 (2013); 10.1063/1.4816648

Precise magnetoresistance and Hall resistivity measurements in the diamond anvil cell
Rev. Sci. Instrum. **75**, 5010 (2004); 10.1063/1.1808045

A novel resistance measurement technique in the field of directional solidification
Rev. Sci. Instrum. **72**, 255 (2001); 10.1063/1.1324737

Resistive and Hall weighting functions in three dimensions
Rev. Sci. Instrum. **69**, 3625 (1998); 10.1063/1.1149149

Sensitivity of resistive and Hall measurements to local inhomogeneities: Finite-field, intensity, and area corrections

Daniel W. Koon,[1,a)] Fei Wang,[2] Dirch Hjorth Petersen,[3] and Ole Hansen[3,4]

[1]*Physics Department, St. Lawrence University, Canton, New York 13617, USA*
[2]*Department of Electronic and Electrical Engineering, South University of Science and Technology of China (SUSTC), Shenzhen 518055, China*
[3]*Department of Micro- and Nanotechnology, Technical University of Denmark, DTU Nanotech, Building 345 East, DK-2800 Kongens Lyngby, Denmark*
[4]*Danish National Research Foundation's Center for Individual Nanoparticle Functionality (CINF), Technical University of Denmark, DK-2800 Kongens Lyngby, Denmark*

We derive exact, analytic expressions for the sensitivity of sheet resistance and Hall sheet resistance measurements to local inhomogeneities for the cases of nonzero magnetic fields, strong perturbations, and perturbations over a finite area, extending our earlier results on weak perturbations. We express these sensitivities for conductance tensor components and for other charge transport quantities. Both resistive and Hall sensitivities, for a van der Pauw specimen in a finite magnetic field, are a superposition of the zero-field sensitivities to both sheet resistance and Hall sheet resistance. Strong perturbations produce a nonlinear correction term that depends on the strength of the inhomogeneity. Solution of the specific case of a finite-sized circular inhomogeneity coaxial with a circular specimen suggests a first-order correction for the general case. Our results are confirmed by computer simulations on both a linear four-point probe array on a large circular disc and a van der Pauw square geometry. Furthermore, the results also agree well with Náhlík *et al.* published experimental results for physical holes in a circular copper foil disc. © *2014 AIP Publishing LLC.* [http://dx.doi.org/10.1063/1.4896947]

I. INTRODUCTION

In a previous paper,[1] we derived expressions for the spatial sensitivity of sheet resistance, R_S, and Hall sheet resistance, $R_H = \mathscr{R}_H B/d$, measurements on a laminar body to local variations in charge transport properties for both van der Pauw[2,3] [vdP] and mobile four-point probe arrays[4,5] [4PP] ($\mathscr{R}_H$ is the Hall coefficient, B is the magnetic flux density, and d is the thickness of the laminar specimen). Those results agree well with previous calculations for sensitivities in a variety of vdP (Refs. 6–9) and 4PP (Refs. 10–13) geometries and with direct experimental results for the sensitivity of the measured sheet resistance, $R_{S,m}$, to inhomogeneities in the local sheet resistance, $R_{S,L}$, for linear 4PPs (Ref. 10) and a square vdP geometry[14] and the sensitivity of the measured Hall sheet resistance, $R_{H,m}$, to local inhomogeneities, $R_{H,L}$, for square and clover vdP geometries.[15]

We expressed these sensitivities in terms of a generalized dimensionless sensitivity[10–12] of the form

$$S_t^T = \frac{A\Delta T/T}{\Delta A(\Delta t/t)},$$

in which the perturbation of a local property t (e.g., $R_{S,L}$ or $R_{H,L}$) alters some macroscopic property, T (e.g., the measured four-wire resistance, $R_{i,m}$, for a particular choice of current and voltage leads for the specimen, as in configurations $i = 1, 2, 5$ for vdP and for $i = A, B, C$ for 4PP in Fig. 1), and A is the area

over which this sensitivity has been normalized. In this formalism, the sensitivity of the measured four-wire resistance to a local variation in sheet resistance can be defined as

$$S_{R_{S,L}}^{R_{i,m}} = A\alpha_i \frac{\partial^2 R_{i,m}}{\partial A \partial R_{S,L}} = A\alpha_i \lim_{\Delta R_{S,L}/R_S \ll 1} \frac{\Delta R_{i,m}}{\Delta A \Delta R_{S,L}},$$

where $\alpha_i = R_S/R_i$ depends on the specimen geometry. Convenient normalization areas, A, are the specimen area for vdP measurements and the square of the probe pitch, p, for 4PP.

For a specimen with a direct sheet conductivity G_S and a Hall sheet conductivity G_H, we calculated the sensitivity of the electric potential, ϕ, to infinitesimal, point-like
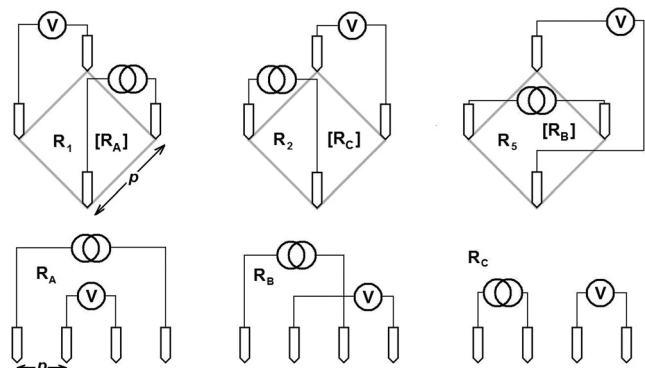
FIG. 1. Principal resistance configurations, R_i, for vdP (i = 1, 2, 5 above) and square 4PP (i = A, B, C above) geometries and for the linear 4PP geometry (below). The distance between adjacent electrodes, or pitch, p, is marked for R_1 above and R_A below. Adapted from Ref. 1. Reprinted with permission from J. Appl. Phys. **114**, 163710 (2013). Copyright 2013 AIP Publishing LLC.

a)Author to whom correspondence should be addressed. Electronic mail: dkoon@stlawu.edu
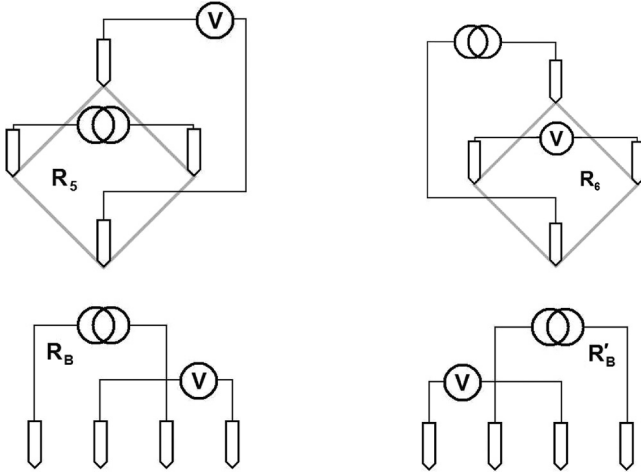
FIG. 2. Two resistance configurations and their reciprocal configurations. Top: the vdP configuration R_5 and its reciprocal configuration, $\tilde{R}_5$. Bottom: the linear 4PP configuration R_B (left) and its reciprocal, $\tilde{R}_B$ (right). The remaining reciprocal configurations, $\tilde{R}_i$, are also obtained by swapping current electrodes for voltage electrodes and vice versa. Reprinted with permission from J. Appl. Phys. **114**, 163710 (2013). Copyright 2013 AIP Publishing LLC.

inhomogeneities, ΔG_S or ΔG_H, in the sheet conductance matrix, **G**, by solving the non-uniform conductance equation

$$\nabla^2 \phi = \frac{\nabla G_S}{G_S} \cdot \mathbf{E} + \mathbf{e_z} \cdot \frac{\nabla G_H}{G_S} \times \mathbf{E} \tag{1}$$

throughout the bulk (except for the current contacts) of the specimen. We took the linear limit by setting the local electric field equal to its unperturbed value, $\mathbf{E} = \mathbf{E}_0$ in Eq. (1), an assumption that clearly falls apart in the extreme cases of a physical hole or a point-like electrical short, for which we need to replace the unperturbed electric field with its perturbed value. Nevertheless, in this linear limit, we find that

$$S_{R_{S,L}}^{R_{i,m}} = \alpha_i A \frac{\partial^2 R_{i,m}}{\partial R_{S,L} \partial A} = \alpha_i A F_i(\mathbf{r})$$
$$= A \frac{\mathbf{J}_{S,i} \cdot \tilde{\mathbf{J}}_{S,i}}{\int \mathbf{J}_{S,i} \cdot \tilde{\mathbf{J}}_{S,i} d\Omega'} = A \frac{\mathbf{E}_i \cdot \tilde{\mathbf{E}}_i}{\int \mathbf{E}_i \cdot \tilde{\mathbf{E}}_i d\Omega'}, \tag{2a}$$

where $\mathbf{J}_S$ is the surface current density and the tilde refers to the "reciprocal" configuration for this geometry, formed by exchanging current leads for voltage leads and vice versa (Fig. 2), and

$$F_i(\mathbf{r}) \equiv [\nabla \mathcal{G}(\mathbf{r}, \mathbf{r}_+) - \nabla \mathcal{G}(\mathbf{r}, \mathbf{r}_-)]$$
$$\times [\nabla \mathcal{G}(\mathbf{r}, \tilde{\mathbf{r}}_+) - \nabla \mathcal{G}(\mathbf{r}, \tilde{\mathbf{r}}_-)] \tag{2b}$$

the product of the difference of gradients of the Green's functions for the sheet resistance, where $\mathbf{r}_+$ and $\mathbf{r}_-$ are the positions of the positive and negative current electrodes and $\tilde{\mathbf{r}}_+$ and $\tilde{\mathbf{r}}_-$ are the positive and negative voltage electrodes. In addition, we calculated

$$S_{R_{H,L}}^{R_{i,m}} = A \frac{\partial^2 R_{i,m}}{\partial R_{H,L} \partial A} = A K_i(\mathbf{r}) = \frac{A \left(\mathbf{J}_{S,i} \times \tilde{\mathbf{J}}_{S,i} \right) \cdot \mathbf{e_z}}{\int \left(\mathbf{J}_{S,i} \times \tilde{\mathbf{J}}_{S,i} \right) \cdot \mathbf{e_z} d\Omega'}$$
$$= \frac{A \left(\mathbf{E}_i \times \tilde{\mathbf{E}}_i \right) \cdot \mathbf{e_z}}{\int \left(\mathbf{E}_i \times \tilde{\mathbf{E}}_i \right) \cdot \mathbf{e_z} d\Omega'} \tag{3a}$$

for the Hall sheet resistance, with

$$K_i(\mathbf{r}) = [\nabla \mathcal{G}(\mathbf{r}, \mathbf{r}_+) - \nabla \mathcal{G}(\mathbf{r}, \mathbf{r}_-)]$$
$$\times [\nabla \mathcal{G}(\mathbf{r}, \tilde{\mathbf{r}}_+) - \nabla \mathcal{G}(\mathbf{r}, \tilde{\mathbf{r}}_-)] \cdot \mathbf{e_z}. \tag{3b}$$

This is the function we called $G_i(\mathbf{r})$ in Ref. 1. We have changed our notation to minimize confusion between this quantity, the conductance tensor, and the Green's functions. This is a linear result in that the change in $R_{i,m}$ is linear in B, ΔA, and either $R_{S,L}$ or $R_{H,L}$. Any extension of Eqs. (2) and (3) to the more general case has to consider what happens as each of these quantities increases beyond the infinitesimal limit. Note Eqs. (2a) and (3a) are intimately related to Eqs. (2) and (3) of Paul and Cornils,[16] who also show the derivation of these expressions.

II. FINITE MAGNETIC FIELD CORRECTION

First we consider Eq. (1) when a finite external magnetic field is applied perpendicular to the specimen while maintaining the same current density at the current source and drain, and $(J_S)_\perp = 0$ along the specimen boundaries. The general problem of calculating field-dependence for F_i and K_i for measurements on a finite specimen is beyond the scope of this paper, but it simplifies in the two limits of a 4PP on an infinite plane (i.e., no finite boundaries) and in the vdP case (i.e., probes are at the boundary of the specimen). For these two limiting cases,

$$F_{i,B} = \frac{\mathbf{J}_{S,i}(\mathbf{B}) \cdot \tilde{\mathbf{J}}_{S,i}(-\mathbf{B})}{\int_\Omega \mathbf{J}_{S,i}(\mathbf{B}) \cdot \tilde{\mathbf{J}}_{S,i}(-\mathbf{B}) d\Omega'} = \begin{cases} F_{i,0} & \text{infinite sheet} \\ F_{i,0} \cos 2\Theta_H + K_{i,0} \sin 2\Theta_H & \text{vdP geometry,} \end{cases}$$
$$K_{i,B} = \frac{\mathbf{J}_{S,i}(\mathbf{B}) \times \tilde{\mathbf{J}}_{S,i}(-\mathbf{B}) \cdot \mathbf{e_z}}{\int_\Omega \mathbf{J}_{S,i}(\mathbf{B}) \times \tilde{\mathbf{J}}_{S,i}(-\mathbf{B}) \cdot \mathbf{e_z} d\Omega'} = \begin{cases} K_{i,0} & \text{infinite sheet} \\ K_{i,0} \cos 2\Theta_H - F_{i,0} \sin 2\Theta_H & \text{vdP geometry.} \end{cases} \tag{4}$$

Here, the Hall angle, Θ_H, is defined by $\tan \Theta_H = R_H/R_S = G_H/G_S$ and second order effects appearing for large Θ_H are not included. We have verified Eq. (4) algebraically for arbitrary placement of electrodes along the edge of a

semi-infinite plane, and thus for any vdP geometry, because it can be mapped to the semi-infinite plane[2,3] by conformal mapping. We have also confirmed Eq. (4) numerically for a vdP square specimen.

III. FINITE INTENSITY CORRECTION

One effect of an inhomogeneity of nonzero intensity, $\Delta G_S/G_S$, in the direct sheet conductance, G_S, is a change in the local electric field in Eq. (1) at the location of the perturbation. For the same perturbation in G_S and G_H (the Hall conductance) as in Sec. II, one can calculate this electric field inside an infinitesimal circular perturbation of radius a in the same way as for a dielectric cylinder or sphere in a uniform electric field.[17] In the present case, the normal surface current density and the tangential electric field are continuous across the edge of the perturbation:

$$(\mathbf{J_S})_\perp = (\mathbf{J_S})_r = G_S\mathbf{E}_r + G_H\mathbf{E}_\theta \quad \mathbf{E}_{||} = \mathbf{E}_\theta,$$

where $\mathbf{J}_S$ is the surface current density. Parallel and perpendicular subscripts are with respect to the boundary between the perturbed and unperturbed regions. If the area of this point-like perturbation vanishes, then this problem is equivalent to an infinitely large specimen, for which the electric field approaches the unperturbed electric field, $\mathbf{E}_0$, sufficiently far from the perturbation. Matching $E_{||}$ yields

$$\phi(r) = \begin{cases} -C_1 r\cos\theta - C_2 r\sin\theta & r < a \\[2ex] \left[-E_0\left(r - \dfrac{a^2}{r}\right) - \dfrac{C_1 a^2}{r}\right]\cos\theta - \left(\dfrac{C_2 a^2}{r}\right)\sin\theta & r > a, \end{cases} \tag{5}$$

where the angle θ is measured with respect to the direction of $\mathbf{E}_0$, while matching $(\mathbf{J}_S)_\perp$ gives us

$$C_1 = \frac{1 + \dfrac{1}{2}\dfrac{\Delta G_S}{G_S}}{\left[1 + \dfrac{1}{2}\dfrac{\Delta G_S}{G_S}\right]^2 + \dfrac{1}{4}\left[\dfrac{\Delta G_H}{G_S}\right]^2}E_0 \quad C_2 = \frac{\dfrac{1}{2}\dfrac{\Delta G_H}{G_S}}{\left[1 + \dfrac{1}{2}\dfrac{\Delta G_S}{G_S}\right]^2 + \dfrac{1}{4}\left[\dfrac{\Delta G_H}{G_S}\right]^2}E_0,$$

or

$$\mathbf{E} = \frac{\left[1 + \dfrac{1}{2}\dfrac{\Delta G_S}{G_S}\right]\mathbf{E}_0 + \dfrac{1}{2}\dfrac{\Delta G_H}{G_S}\hat{\mathbf{e}}_z \times \mathbf{E}_0}{\left[1 + \dfrac{1}{2}\dfrac{\Delta G_S}{G_S}\right]^2 + \dfrac{1}{4}\left[\dfrac{\Delta G_H}{G_S}\right]^2} = \frac{C_1}{E_0}\mathbf{E}_0 + \frac{C_2}{E_0}\hat{\mathbf{e}}_z \times \mathbf{E}_0. \tag{6}$$

In the special case of $G_H = 0 = \Delta G_H$, the local electric field reduces to $\mathbf{E} = \mathbf{E}_0/\left(1 + \frac{1}{2}\frac{\Delta G_S}{G_S}\right)$, and since ΔR_i is proportional to the product of both $\frac{\Delta G_S}{G_S^2}$ and $\mathbf{E}$

$$S_{R_{S,L}}^{R_{i,m}} = S_{R_{S,L}}^{R_{i,m}}\bigg|_{\frac{\Delta R_S}{R_S}=0}\bigg/\left(1 - \varepsilon\frac{\Delta R_S}{R_S}\right) \tag{7}$$

with $\varepsilon = 1/2$, and where we have used the fact that $\Delta G_S/G_S \cong -\Delta R_S/R_S$ when $\Delta G_S/G_S \ll 1$. Discrepancy of the nonlinearity constant in the denominator of Eq. (7) with $\varepsilon = 0.68\pm0.02$ based on laboratory simulations for a square vdP specimen with electric contacts at the corners[9] may be due to the intrinsically nonzero area, $\Delta A/A$, of a perturbation in a finite resistor simulation.

Inserting Eq. (6) into Eq. (1), we find the effect of the local point perturbation in conductance

$$\nabla^2\phi = -\frac{I}{G_S}\left[\delta(\mathbf{r} - \mathbf{r}_+) - \delta(\mathbf{r} - \mathbf{r}_-)\right] + \Delta A\left[\frac{\Delta G_S}{G_S}\frac{C_1}{E_0} + \frac{\Delta G_H}{G_S}\frac{C_2}{E_0}\right]\left[\nabla\delta(\mathbf{r} - \mathbf{r}_0)\cdot\mathbf{E}_0\right]$$

$$+\Delta A\left[\frac{\Delta G_H}{G_S}\frac{C_1}{E_0} - \frac{\Delta G_S}{G_S}\frac{C_2}{E_0}\right]\left[\mathbf{e_z}\cdot\nabla\delta(\mathbf{r} - \mathbf{r}_0)\times\mathbf{E}_0\right],$$

and so the resultant effect on the measured four-wire resistance is

$$\Delta R_{i,m} = -\frac{\Delta A}{G_S}\left\{\left[\frac{\Delta G_S}{G_S}\frac{C_1}{E_0} + \frac{\Delta G_H}{G_S}\frac{C_2}{E_0}\right]F_i - \left[\frac{\Delta G_H}{G_S}\frac{C_1}{E_0} - \frac{\Delta G_S}{G_S}\frac{C_2}{E_0}\right]K_i\right\}$$

$$= -\frac{\Delta A}{G_S}\left[\frac{\dfrac{\Delta G_S}{G_S} + \dfrac{1}{2}\left[\left(\dfrac{\Delta G_S}{G_S}\right)^2 + \left(\dfrac{\Delta G_H}{G_S}\right)^2\right]}{\left(1 + \dfrac{1}{2}\dfrac{\Delta G_S}{G_S}\right)^2 + \dfrac{1}{4}\left(\dfrac{\Delta G_H}{G_S}\right)^2}F_i - \frac{\dfrac{\Delta G_H}{G_S}}{\left(1 + \dfrac{1}{2}\dfrac{\Delta G_S}{G_S}\right)^2 + \dfrac{1}{4}\left(\dfrac{\Delta G_H}{G_S}\right)^2}K_i\right], \tag{8}$$

and the sensitivities to G_S and G_H are

$$S_{G_S}^{R_i}\Big|_{\Delta G_H=0} = \frac{A(\Delta R_i/R_i)}{\Delta A(\Delta G_S/G_S)}\Big|_{\Delta G_H=0}$$

$$= -A\alpha_i \frac{1}{1+\left(\dfrac{G_H}{G_S}\right)^2} \cdot \frac{F_{i,B}}{1+\dfrac{1}{2}\dfrac{\Delta G_S}{G_S}} \quad \text{and}$$

$$S_{G_H}^{R_i}\Big|_{\Delta G_S=0} = \frac{A(\Delta R_i/R_i)}{\Delta A(\Delta G_H/G_H)}\Big|_{\Delta G_S=0}$$

$$= A \frac{\dfrac{G_H}{G_S}}{1+\left(\dfrac{G_H}{G_S}\right)^2} \cdot \frac{K_{i,B}-\dfrac{1}{2}\dfrac{\Delta G_H}{G_S}F_{i,B}}{1+\dfrac{1}{4}\left(\dfrac{\Delta G_H}{G_S}\right)^2}. \tag{9}$$

Here, we have used the difference equation for $S_t^{R_i}$ rather than the differential form, since it allows us to calculate the difference relative to zero perturbation. The "B" subscripts for F_i and K_i in Eq. (9) mean that these quantities must be calculated for the appropriate magnetic flux density, B.

IV. FINITE-AREA CORRECTION

The analysis of the Sec. III, in which the specimen's borders were assumed to vanish, gives an exact solution for the limiting case in which the electrode spacing is much less than the dimensions of the specimen (i.e., a 4PP on an infinite conducting plane), but it fails to match the nonlinearity we notice in the work of Náhlik *et al.*[18] when the area of the inhomogeneity increases. This suggests a correction to Eq. (9) as a function of $\Delta A/A$. In Eq. (5) above, we assumed an infinite conducting plane in the form of the perturbation to the electric field due to the inhomogeneity. If instead, we assume a circular specimen of unit radius, with a coaxial circular inhomogeneity of radius a, the local electric potential will be

$$\phi(r) = \begin{cases} \displaystyle\sum_{n=1}^{\infty} r^n(1+a^{-2n})(A_n\cos\theta + B_n\sin\theta) & r < a \\ \displaystyle\sum_{n=1}^{\infty} (r^n + r^{-n})(A_n\cos\theta + B_n\sin\theta) & r > a \end{cases}$$

for constants A_n and B_n, such that the normal surface current densities vanish on the specimen boundary. Furthermore, if we define θ such that it points in the direction of the unperturbed local electric field, then $B_n = 0$ for all n and $A_n = 0$ for all $n \neq 1$. The effect of a specimen of noncircular shape, or of an inhomogeneity or either noncircular shape or of noncoaxial location is to add quadrupole and higher terms to this dipole term in Eq. (5). For the case of inhomogeneities in the sheet resistance but not the Hall sheet resistance,

$$S_{R_{S,L}}^{R_{i,m}} \rightarrow S_0 \left(\frac{1+\dfrac{\gamma}{2}(\Delta A/A)}{1+\dfrac{\gamma}{2}(1+\Delta A/A)} \right) \tag{10}$$

to lowest order, where we have introduced $\gamma = \Delta G_S/G_S$, S_0 is the value of the sensitivity in the linear limit of infinitesimal B field, area, and strength of the perturbation (Eqs. (2) and (3)). In the limit of $\Delta A/A \ll 1$ and $\Delta G_S/G_S \ll 1$, this reduces to the $S_0\left(1+\frac{1}{2}\Delta G_S/G_S\right)^{-1} \approx S_0\left(1-\frac{1}{2}\Delta R_S/R_S\right)^{-1}$ of Eq. (7).

The most extreme perturbations are electric "short circuits" ($\Delta R_{S,L}/R_S = -1$) or "open circuits" consisting of
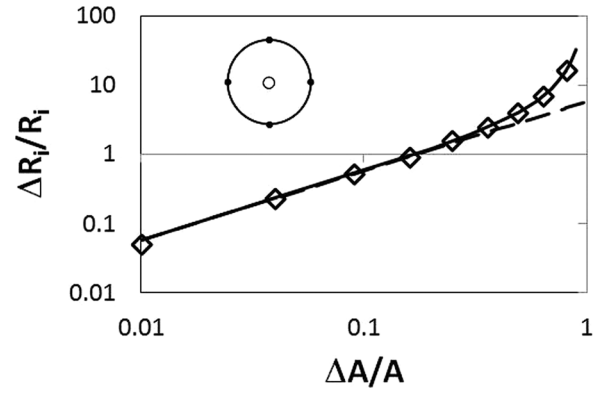

FIG. 3. Impact of a hole of area ΔA in the center of a circular vdP specimen of area A (inset) on the measured four-wire resistance, R_i. Diamonds represent experimental data from Náhlik *et al.*[18] on 25 mm diameter, 35 μm thick copper foil specimens. Data for both configuration 1 and the dual configuration are indistinguishable on the original graph. The dashed line represents a least-square linear fit to the first four data points to the left with Eq. (9). Although strictly valid only for areas $\Delta A/A \ll 1$, it provides an error of less than 10% for holes with diameters up to nearly 40% of the overall diameter of the disc. The solid line represents the analytical theoretical prediction of Eq. (11).

physical holes, with the latter producing twice the effect on the measured resistance as predicted by the linear weighting function (Eq. (2)). We have applied the linear correction of Eq. (9) to the data from Náhlik *et al.* experimental study of the effects of a finite hole in the center of a circular disc of copper foil[18] as shown in Fig. 3. This calculation provides less than 10% error for $\Delta A/A < 0.15$. While the nonlinear expression (Eq. (10), not shown on graph) improves the fit somewhat, it is not sufficient to correct the fit.

But this system can also be solved analytically (Appendix), with

$$\frac{\Delta R_i}{R_i} = -\frac{4}{\ln 2}\sum_{n=1,3,5,\dots}^{\infty} \frac{(\Delta A/A)^n}{n}\bigg/\left[1-\left(\frac{\Delta A}{A}\right)^{2n}\right] \tag{11}$$

shown in Figure 3 as a solid curve indistinguishable from Eq. (10) with a sheet resistance fit of 584 $\mu\Omega$, fitting in the range of 580–606 $\mu\Omega$ reported for the foil. A straight, dashed line represents the linear fit (Eq. (9)), with a least-squares best fit value of $S_{R_{S,L}}^{R_{i,m}} = 5.772$, agreeing to four figures with twice 2/ln2, the *linear* result from the equations in Ref. 1, and in agreement with Eq. (7) for $\varepsilon = 1/2$. Although the linear limit (Eq. (9)) is strictly valid only for areas $\Delta A/A \ll 1$, it provides an acceptable fit to theory up to about $\Delta A/A \leq 0.15$, a hole with a diameter nearly 40% of the diameter of the disc, where it provides an error of less than 10%.

V. SENSITIVITY TO TRANSPORT QUANTITIES

The sensitivities to local perturbations in the materials properties, R_S and either R_H or $\tan\Theta_H$, or in the transport properties sheet carrier density N_S, carrier mobility μ, and B are usually more relevant to laboratory measurement than the sensitivities to G_S and G_H. While the general problem of calculating the nonlinearity when more than one of these variables is allowed to vary is quite daunting, the behavior when a single variable, t, is allowed to vary, e.g., $t = N_S$, μ, or B, while the others remain fixed, is straightforward

$$S_t^T = S_{G_S}^T \frac{\partial G_S}{\partial t}\bigg|_{\Delta G_H = 0} + S_{G_H}^T \frac{\partial G_H}{\partial t}\bigg|_{\Delta G_S = 0}.$$

And so we have,

$$S_{N_{S,L}}^{R_{i,m}}\bigg|_{\substack{\Delta B = 0 \\ \Delta \mu = 0}} = A\alpha_i \begin{cases} \dfrac{-\left[1 + \dfrac{1 + \mu^2 B^2}{2}\dfrac{\Delta N_S}{N_S}\right] F_{i,B} + \mu B K_{i,B}}{(1 + \mu^2 B^2)\left[\left(1 + \dfrac{1}{2}\dfrac{\Delta N_S}{N_S}\right)^2 + \left(\dfrac{1}{2}\dfrac{\Delta N_S}{N_S}\mu B\right)^2\right]} & \text{general case} \\[2em] \dfrac{-\cos\Theta_H F_{i,0} - \dfrac{1}{2}\dfrac{\Delta N_S}{N_S}F_{i,B}}{\left(1 + \dfrac{1}{2}\dfrac{\Delta N_S}{N_S}\right)^2 + \left(\dfrac{1}{2}\dfrac{\Delta N_S}{N_S}\tan\Theta_H\right)^2} & \text{vdP} \end{cases}$$

$$S_{\mu_L}^{R_{i,m}}\bigg|_{\substack{\Delta B = 0 \\ \Delta N_S = 0}} = A\alpha_i \begin{cases} \dfrac{-(1 - \mu^2 B^2)F_{i,B} + 2\mu B K_{i,B}}{(1 + \mu^2 B^2)^2\left(1 + \dfrac{1}{2}\dfrac{\Delta\mu}{\mu}\right)} & \text{general case} \\[2em] \dfrac{-\cos^2\Theta_H F_{i,0}}{1 + \dfrac{1}{2}\dfrac{\Delta\mu}{\mu}} & \text{vdP} \end{cases} \qquad (12)$$

$$S_{B_L}^{R_{i,m}}\bigg|_{\substack{\Delta N_S = 0 \\ \Delta \mu = 0}} = A\alpha_i \begin{cases} \mu B \dfrac{\left[1 - \mu^2 B^2\left(1 + \dfrac{\Delta B}{B}\right)\right]K_{i,B} + 2\mu B\left[1 + \dfrac{1}{4}\dfrac{\Delta B}{B}(1 - \mu^2 B^2)\right]F_{i,B}}{(1 + \mu^2 B^2)^2\left(1 + \dfrac{1}{4}\mu^2\Delta B^2\right)} & \text{general case} \\[2em] \dfrac{1}{2}\sin 2\Theta_H \dfrac{K_{i,0} - \dfrac{\mu\Delta B}{2}F_{i,0}}{1 + \dfrac{1}{4}\mu^2\Delta B^2}. & \text{vdP.} \end{cases}$$

For the case of a 4PP in an infinite plane, we can substitute $F_{i,B} = F_{i,0}$ and $K_{i,B} = K_{i,0}$. Interestingly, when Eq. (4) is combined with the above, the low-field, low-perturbation limit yields

$$\lim_{\frac{\Delta N_S}{N_S}, \frac{\Delta B}{B}, \mu B \ll 1} S_{N_{S,L}}^{R_{i,m}}\bigg|_{\substack{\Delta B = 0 \\ \Delta \mu = 0}} = A\alpha_i \begin{cases} -F_{i,0} + \mu B K_{i,0} & \text{4PP : infinite plane} \\ -F_{i,0} - \mu B K_{i,0} & \text{vdP} \end{cases}$$

$$\lim_{\frac{\Delta\mu}{\mu}, \frac{\Delta B}{B}, \mu B \ll 1} S_{\mu_L}^{R_{i,m}}\bigg|_{\substack{\Delta B = 0 \\ \Delta N_S = 0}} = A\alpha_i \begin{cases} -F_{i,0} + 2\mu B K_{i,0} & \text{4PP : infinite plane} \\ -F_{i,0} & \text{vdP} \end{cases} \qquad (13)$$

$$\lim_{\frac{\Delta\mu}{\mu}, \frac{\Delta N_S}{N_S}, \mu B \ll 1} S_{B_L}^{R_{i,m}}\bigg|_{\substack{\Delta B = 0 \\ \Delta N_S = 0}} = A\alpha_i \begin{cases} \mu B[K_{i,0} + 2\mu B F_{i,0}] & \text{4PP : infinite plane} \\ \mu B K_{i,0} & \text{vdP} \end{cases}$$

to lowest order in μB. This difference between the 4PP and vdP cases is confirmed in Figs. 4 and 5 for the 4PP geometry using Comsol simulation and for vdP in a finite-difference relaxation simulation on a 101×101 grid in Excel, for fields corresponding to Hall angles of $\tan\Theta_H = \mu_H B = 0, 0.02$, and 0.04 in both cases.

The 4PP case (Fig. 4) models a conducting plane of radius $100p$ with $qN_S = 0.25\,\text{C/m}^3$, $\mu = 0.004\,\text{m}^2/\text{V}\cdot\text{s}$ and the perturbation placed at $(x, y) = (-0.4p, +0.1p)$. The best fit to Eqs. (12) and (13) was achieved with $S_{R_{S,L}}^{R_{B,m}} = \alpha_B A F_{B,0} = 1.5717$ and $S_{R_{H,L}}^{R_{H,m}} = \alpha_B A K_{B,0} = 1.447$, while exact calculation from Ref. 1 yields 1.57132 and 1.47211, respectively, in remarkable agreement, considering the finite area of the perturbation and its proximity to the singularity at $(-0.5p, 0)$. Values for sensitivities from the simulation and fit agree to within 0.001 for all data points in the main plot. The Comsol results were indistinguishable when the boundary was either grounded or insulating.

The vdP case (Fig. 5) models a square specimen of side a with electrodes at each corner. A perturbation is placed at a distance $(x, y) = (0.3a, 0.5a)$ from one current electrode, and the same distance from the adjacent voltage lead. Fitting parameters in Eqs. (10) and (12) were $F_{1,0} = 1.465$ and $K_{1,0} = -2.8428$. The deviations of up to 3% in the simulation data from theory as μB increases (bottom line of the inset to Fig. 5) seem to be due to discretization effects of the 101×101 grid.

Figs. 4 and 5 clearly match Eq. (13), i.e. the difference in the B-field dependence of the resistive sensitivities in the two limits of vdP geometry and the infinite-plane 4PP is clearly seen, and they also show the effects of Eq. (4), the contrast between the B-dependence of F_i and K_i for the vdP geometry and the B-independence of these quantities for the infinite-plane 4PP.

Finally, we can express the sensitivity of charge transport measurements to variations in their own local values in the non-linear regime, perhaps the most practical representation in the laboratory. The effects of perturbations in either $R_{S,L}$ or $R_{H,L}$ (while keeping the other parameter fixed) are

$$
S_{R_{S,L}}^{R_{i,m}}\Big|_{\Delta R_H=0} = A\alpha_i
\begin{cases}
\dfrac{\left[1-\left(\dfrac{R_H}{R_S}\right)^2\right]F_{i,B}+2\dfrac{R_H}{R_S}K_{i,B}}{\left[1+\left(\dfrac{R_H}{R_S}\right)^2\right]\left(1+\dfrac{1}{2}\dfrac{\Delta R_S}{R_S}\right)} & \text{general case}\\[4ex]
\dfrac{\cos^2\Theta_H F_{i,0}}{1+\dfrac{1}{2}\dfrac{\Delta R_S}{R_S}} & \text{vdP}
\end{cases}
$$

$$
S_{R_{H,L}}^{R_{i,m}}\Big|_{\Delta R_S=0} = A\alpha_i
\begin{cases}
\dfrac{R_H}{R_S}\dfrac{\left[1-\left(\dfrac{R_H}{R_S}\right)^2\left(1+\dfrac{\Delta R_H}{R_S}\right)\right]K_{i,B}+\left\{2\dfrac{R_H}{R_S}+\dfrac{1}{2}\dfrac{\Delta R_H}{R_S}\left[1-\left(\dfrac{R_H}{R_S}\right)^2\right]\right\}F_{i,B}}{\left[1+\left(\dfrac{R_H}{R_S}\right)^2\right]\left[1+\dfrac{1}{4}\left(\dfrac{\Delta R_H}{R_S}\right)^2\right]} & \text{general case}\\[4ex]
\dfrac{1}{2}\sin 2\Theta_H\dfrac{K_{i,0}+\dfrac{1}{2}\dfrac{\Delta R_H}{R_S}F_{i,0}}{1+\dfrac{1}{4}\left(\dfrac{\Delta R_H}{R_S}\right)^2}, & \text{vdP,}
\end{cases}
\tag{14}
$$

and for perturbations in either R_S or $\tan\Theta_H$ is

$$
S_{R_{S,L}}^{R_{i,m}}\Big|_{\Delta\tan\Theta_H=0} = A\alpha_i
\begin{cases}
\dfrac{(\cos 2\Theta_H F_{i,B}+\sin 2\Theta_H K_{i,B})\cos\Theta_H\left(1+\dfrac{1}{2}\cos\Theta_H\dfrac{\Delta R_S}{R_S}\right)}{1+\dfrac{\Delta R_S}{R_S}+\dfrac{1}{4}\left(\dfrac{\Delta R_S}{R_S}\right)^2(1+\tan^2\Theta_H)} & \text{general case}\\[4ex]
\dfrac{F_{i,0}\cos\Theta_H\left(1+\dfrac{1}{2}\cos\Theta_H\dfrac{\Delta R_S}{R_S}\right)}{1+\dfrac{\Delta R_S}{R_S}+\dfrac{1}{4}\left(\dfrac{\Delta R_S}{R_S}\right)^2(1+\tan^2\Theta_H)} & \text{vdP}
\end{cases}
$$

$$
S_{\tan\Theta_{H,L}}^{R_{i,m}}\Big|_{\Delta R_S=0} = A\alpha_i
\begin{cases}
\dfrac{1}{2}\sin 2\Theta_H\dfrac{\left\{\left[2\tan\Theta_H+\dfrac{1}{2}\Delta\tan\Theta_H(1-\tan^2\Theta_H)\right]F_{i,B}+\left[1-\tan^2\Theta_H\left(1+\dfrac{\Delta\tan\Theta_H}{\tan\Theta_H}\right)\right]K_{i,B}\right\}}{1+\dfrac{1}{4}(\Delta\tan\Theta_H)^2} & \text{general case}\\[4ex]
\dfrac{1}{2}\sin 2\Theta_H\dfrac{K_{i,0}+\dfrac{1}{2}\Delta\tan\Theta_H F_{i,0}}{1+\dfrac{1}{4}(\Delta\tan\Theta_H)^2} & \text{vdP.}
\end{cases}
\tag{15}
$$

All expressions in Eqs. (14) and (15) are exact to all orders of either $\Delta R_{S,L}/R_S$ or $\Delta R_{H,L}/R_H$ (although only in the small-area limit) and have been confirmed using the Excel spreadsheet simulation for a vdP square specimen with electrodes at its corners. It is interesting that the expressions for the two cases can always be reduced to just two functions, the zero-magnetic-field functions, $F_{i,0}$ and $K_{i,0}$, simplifying and speeding up calculations for the general case on a specific specimen.
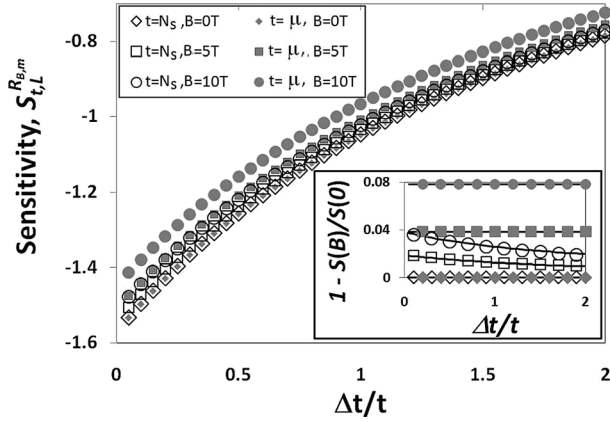
FIG. 4. Variation of sensitivities $S_{N_{S,L}}^{R_{B,m}}\big|_{\substack{\Delta B = 0 \\ \Delta\mu = 0}}$ and $S_{\mu_L}^{R_{B,m}}\big|_{\substack{\Delta B = 0 \\ \Delta N_S = 0}}$ with $\Delta N_S/N_S$ and $\Delta\mu/\mu$, for fields of 0, 5 T, and 10 T for Comsol simulation of a linear 4PP probe with pitch p in configuration B on a conducting plane of radius $100p$, with $qN_S = 0.25\,\text{C/m}^3$, $\mu = 0.004\,\text{m}^2/(\text{V}\cdot\text{s})$, and the perturbation placed at $(x,y) = (-0.4p, +0.1p)$. Simulation and fit agree to within 0.1% for all data points in the main plot.

VI. CONCLUSIONS

Extending the linear results of Ref. 1 for the sensitivity of charge transport measurements to nonlinear regimes yields exact analytic expressions for both finite magnetic fields in the vdP and 4PP limits and strong perturbations on an infinitesimal area, but as yet the finite-area sensitivity can only be approximated by solving the boundary-value problem for the specific inhomogeneity. Magnetic fields have no effect on sensitivities in the limit of the infinite conducting plane but mix zero-field resistive and Hall sensitivities for vdP measurements; strong inhomogeneities introduce a nonlinear correction that depends only on the strength and area, in the limit of infinitesimal area. Our calculations for strong inhomogeneities match published reports for vdP copper foil specimens[18] and our calculations for combined finite magnetic field and finite strength match computer simulations for both vdP and 4PP specimens.
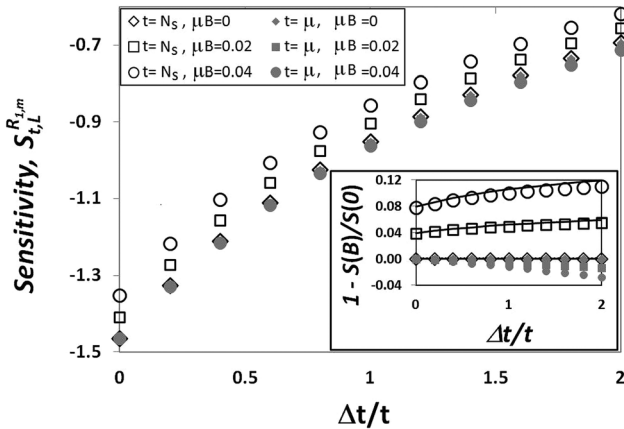

FIG. 5. Variation of weighting functions, $F_1 = S_{N_{S,L}}^{R_{1,m}}\big|_{\Delta B, \Delta\mu = 0}$ and $S_{\mu_L}^{R_{1,m}}\big|_{\Delta B, \Delta N_S = 0}$ with $\Delta N_S/N_S$ and $\Delta\mu/\mu$, for Hall angles $\tan\Theta_H = \mu B = 0, 0.02, 0.04$ (i.e., $\mu = 1$ in dimensionless units) for a 101×101 Excel simulation on a square vdP specimen of side a with the perturbation at a distance $(x, y) = (0.3a, 0.5a)$ from one current electrode, equidistant from the other. Fitting parameters in Eqs. (10) and (13) were $F_{1,B=0} = 1.465$ and $K_{1,B=0} = -2.8428$. The simulation data differ from theory by up to 3% with increasing μB (bottom line of inset).

Analysis of sensitivity provides a powerful, visual, and intuitive tool for understanding how local inhomogeneities can have undue influence on a measurement and for understanding how to prevent that from happening.

APPENDIX: EXACT SOLUTION FOR THE ANNULAR DISC

For an unperturbed unit circular disc centered at the origin and having a uniform conductance, G_S, and a current, I, entering the specimen via a point contact at the edge at $\theta = +3\pi/4$ and exiting at the edge at $\theta = -3\pi/4$, the electric potential can be written in series expansion as

$$\Phi_0(r, \theta) = \frac{2I}{\pi G_S} \sum_{n=1}^{\infty} \frac{r^n}{n} \sin\frac{3n\pi}{4} \sin n\theta$$

for $0 \le r \le 1$, with a corresponding four-wire resistance of $R_0 = I\ln 2/\pi G_S$ for pointlike voltage probes located at the edge at $\theta = \pm\pi/4$, in agreement with van der Pauw's equation[2,3] for a symmetric specimen.

The electric potential inside an annular disc with the same electrodes but an inner radius, s, can be written as a correction to the above form

$$\Phi = \Phi_0 + \Phi_1,$$

subject to the boundary conditions

$$\frac{\partial\Phi}{\partial r}\bigg|_{r=s} = 0 \quad \text{and} \quad \frac{\partial\Phi_1}{\partial r}\bigg|_{r=1} = 0.$$

The perturbation and the total potential that satisfy these conditions can be expressed as

$$\Phi_1(r, \theta) = \frac{2I}{\pi G_S} \sum_{n=1}^{\infty} \frac{1}{n} \frac{s^{2n}\sin(3n\pi/4)}{1 - s^{2n}}(1 + r^{-2n})r^n \sin n\theta, \text{ and}$$

$$\Phi(r, \theta) = \frac{2I}{\pi G_S} \sum_{n=1}^{\infty} \frac{r^n}{n}\left[\frac{1 + s^{2n}r^{-2n}}{1 - s^{2n}}\right]\sin\frac{3n\pi}{4}\sin n\theta,$$

and the relative change in the four-wire resistance as

$$\frac{\Delta R}{R_0} = -\frac{8}{\ln 2}\sum_{n=1,2,3,}^{\infty} \frac{1}{n}\frac{s^{2n}}{1 - s^{2n}}\sin\frac{n\pi}{4}\sin\frac{3n\pi}{4}$$

$$= -\frac{4}{\ln 2}\sum_{n=1,3,5,\ldots}^{\infty} \frac{(\Delta A/A)^n}{n}\bigg/\left[1 - \left(\frac{\Delta A}{A}\right)^{2n}\right],$$

or Eq. (11) above, in which the odd terms (n = odd) in the first expression have been combined with the "2n" terms to eliminate the $\sin(n\pi/4)\sin(3n\pi/4)$ factor.

[1] D. W. Koon, F. Wang, D. H. Petersen, and O. Hansen, J. Appl. Phys. **114**, 163710 (2013).

[2] L. J. van der Pauw, Philips Res. Rep. **13**, 1 (1958).

[3] L. J. van der Pauw, Philips Tech. Rev. **20**, 220 (1958).

[4] L. B. Valdes, Proc. IRE **42**, 420 (1954).

[5] F. M. Smits, Bell Syst. Tech. J. **37**, 711 (1958).

[6] D. W. Koon and C. J. Knickerbocker, Rev. Sci. Instrum. **63**, 207 (1992).

[7] D. W. Koon and C. J. Knickerbocker, Rev. Sci. Instrum. **64**, 510 (1993).

[8] D. W. Koon and C. J. Knickerbocker, Rev. Sci. Instrum. **67**, 4282 (1996).

[9] D. W. Koon, Rev. Sci. Instrum. **77**, 094703 (2006).

[10] D. H. Petersen, R. Lin, T. M. Hansen, E. Rosseel, W. Vandervorst, C. Markvardsen, D. Kjær, and P. F. Nielsen, J. Vac. Sci. Technol. B **26**, 362 (2008).

[11] F. Wang, D. H. Petersen, T. M. Hansen, T. R. Henriksen, and P. Bøggild, J. Vac. Sci. Technol. B **28**, C1C34 (2010).

[12] F. Wang, D. H. Petersen, F. W. Osterberg, and O. Hansen, in *Proceedings of the 17th IEEE International Conference on Advanced Thermal Processing of Semiconductors, RTP 2009* (IEEE, New York, 2009) p. 151.

[13] D. H. Petersen, O. Hansen, P. Bøggild, R. Lin, P. F. Nielsen, D. Lin, C. Adelmann, A. Alian, C. Merckling, J. Penaud, G. Brammertz, J. Goossens, W. Vandervorst, and T. Clarysse, J. Vac. Sci. Technol. B **28**, C1C41 (2010).

[14] D. W. Koon and W. K. Chan, Rev. Sci. Instrum. **69**, 4218 (1998).

[15] J. K. Scherschligt and D. W. Koon, Rev. Sci. Instrum. **71**, 587 (2000).

[16] O. Paul and M. Cornils, Appl. Phys. Lett. **95**, 232112 (2009).

[17] J. D. Jackson, *Classical Electrodynamics*, 2nd ed. (John Wiley & Sons, New York, 1975), p. 149.

[18] J. Náhlík, I. Kašpárková, and P. Fitl, Measurement **44**, 1968 (2011).